Fluorescence Correlation Spectroscopy of Labeled Azurin Reveals Photoinduced Electron Transfer between Label and Cu Center

Andreoni, A.; Sen, S.; Hagedoorn, P.-L.; Buma, W.J.; Aartsma, T.J.; Canters, G.W.

DOI
10.1002/chem.201703733

Publication date
2018

Document Version
Final published version

Published in
Chemistry-A European Journal

ChemPubSoc Europe

DOI: 10.1002/chem.201703733

CHEMISTRY A European Journal Full Paper

Electron Transfer

Fluorescence Correlation Spectroscopy of Labeled Azurin Reveals Photoinduced Electron Transfer between Label and Cu Center

Alessio Andreoni[+],[a, d] Saptaswa Sen[+],[a, e] Peter-Leon Hagedoorn,[b] Wybren J. Buma,[c] Thijs J. Aartsma,[a] and Gerard W. Canters*[a]

Abstract: Fluorescent labeling of biomacromolecules enjoys increasing popularity for structural, mechanistic, and microscopic investigations. Its success hinges on the ability of the dye to alternate between bright and dark states. Förster resonance energy transfer (FRET) is an important source of fluorescence modulation. Photo-induced electron transfer (PET) may occur as well, but is often considered only when donor and acceptor are in van der Waals contact. In this study, PET is shown between a label and redox centers in oxidoreductases, which may occur over large distances. In the small blue copper protein azurin, labeled with ATTO655, PET is observed when the label is at 18.5 Å, but not when it is at 29.1 Å from the Cu. For Cu^{II}, PET from label to Cu occurs at a rate of $(4.8\pm0.3)\times10^4\ s^{-1}$ and back at $(0.7\pm0.1)\times10^3\ s^{-1}$. With Cu^{I} the numbers are $(3.3\pm0.7)\times10^6\ s^{-1}$ and $(1.0\pm0.1)\times10^4\ s^{-1}$. Reorganization energies and electronic coupling elements are in the range of 0.8–1.2 eV and 0.02–0.5 cm^{-1}, respectively. These data are compatible with electron transfer (ET) along a through-bond pathway although transient complex formation followed by ET cannot be ruled out. The outcome of this study is a useful guideline for experimental designs in which oxidoreductases are labelled with fluorescent dyes, with particular attention to single molecule investigations. The labelling position for FRET can be optimized to avoid reactions like PET by evaluating the structure and thermodynamics of protein and label.

Introduction

Fluorescent labelling of biomacromolecules has become a popular tool for biochemical, biological and biomedical investigations and the range of applications is still growing. For instance, labelling of two partner proteins with a donor and an acceptor dye allows monitoring their mutual distance in vivo and in vitro as a function of time.[1] In a similar way, structural information can be obtained about conformational dynamics[2] and about the structure of macromolecular complexes.[3] Fluorescent labelling is indispensable for super-resolution microscopy.[4] Fluorescently labelled enzymes have been monitored at the single molecule level during catalytic turnover.[5,6] In all these cases, the dye molecules are continuously excited and deactivated, and understanding the details of the deactivation process is of crucial importance for the proper use of these fluorophores. Two important sources of deactivation are Förster resonance energy transfer (FRET) and photo-induced electron transfer (PET). The theory and the application of FRET have been amply documented.[7] On the other hand, although Gray and co-workers extensively studied electron transfer by photo-excited inorganic complexes across a protein,[8,9] studies of PET involving dye labels have often focused on cases in which the label is in van der Waals contact with nucleotides like guanosine or amino acids like tryptophan or tyrosine.[10–12] Here, we show that PET may occur on a much wider scale in dye-labeled oxidoreductases.

As a model system, the small blue copper protein azurin from *Pseudomonas aeruginosa,* labeled with ATTO655 was chosen (Figure S4). Azurin is a small (14 kDa) blue copper protein that is found in a variety of microorganisms and fulfills a putative role in oxidative stress-induced responses.[13,14] Apart from its stability over a wide range of temperatures, ionic strength, and pH, azurin offers the advantage of its structural and mechanistic properties being well-documented.[13,15] ATTO655 was chosen since its properties have been thorough-

[a] *Dr. A. Andreoni,[+] Dr. S. Sen,[+] Prof. T. J. Aartsma, Prof. G. W. Canters*
Leiden Institute of Physics, Leiden University
Niels Bohrweg 2, 2333CC Leiden (The Netherlands)
E-mail: canters@chem.leidenuniv.nl

[b] *Prof. P.-L. Hagedoorn*
TU Delft, Applied Sciences, Biotechnology, Building 58
Van der Maasweg 9, 2629 HZ Delft (The Netherlands)

[c] *Prof. W. J. Buma*
Van't Hoff Institute for Molecular Sciences
Science Park 904, P.O. Box 94157, 1090 GD Amsterdam (The Netherlands)

[d] *Dr. A. Andreoni[+]*
Present address: National Heart, Lung, and Blood Institute
National Institutes of Health, Bethesda, MD (USA)

[e] *Dr. S. Sen[+]*
Present address: AlbaNova University Center
Department of Applied Physics, KTH-Royal Institute of Technology, 10691 Stockholm (Sweden)

[+] *These authors contributed equally to this work.*

Supporting information and the ORCID identification numbers for the authors of this article can be found under: https://doi.org/10.1002/chem.201703733. The Supporting Information includes absorption, florescence and fluorescence correlation spectroscopy; autocorrelation and data analysis; Rehm–Weller equation; fluorescence anisotropy measurements; cyclic voltammetry; power dependence of f(I); TD-DFT and pathway calculations.

ly analyzed and reported in literature.[16–18] Under aerobic conditions ATTO655 is stable, shows little blinking, and is not easily bleached.[16,17] Therefore the experiments in the present study were performed under aerobic conditions.

The technique chosen here to study the time dependence of the label emission is fluorescence correlation spectroscopy (FCS), a single-molecule technique that can be used to monitor diffusing fluorescent particles in dilute solutions.[19,20] Probing small numbers of molecules at a time by FCS and statistical analysis of the data reveals dynamics otherwise obscured by ensemble averaging.[19,21] When combined with modern hardware and software FCS allows for a time resolution in the ps range.[22] The upper time limit is determined by the residence time of the molecules in the probe volume, which can be increased by changing the viscosity of the solution, or by linking the molecules to bigger, and thereby slower-moving particles.[19,21]

It is helpful to obtain beforehand an idea about the reactions that might contribute to the FCS signal in our case. Apart from the intramolecular electron transfer (ET) between label and Cu center, these reactions could be intermolecular reactions between redox-active components in the solution and a) the excited label or b) the Cu center. The latter reaction can be disregarded: hexacyanoferrate(II) and (III), which have been used in the present study, react with azurin by forming an encounter complex within which ET occurs on a time scale of 20–200 ms.[23] This is much longer than the time an azurin molecule needs on average to traverse the confocal volume (vide infra), which means that these reactions fall outside the observation window of the FCS experiments. The same may be assumed to hold when ascorbate is used as a reductant. Notably, FRET-related processes occur on the ns time scale and are not resolved within the time window of the present FCS experimental set-up.

Thus, for the interpretation of the FCS traces one only needs to consider the intramolecular ET between label and Cu, and the intermolecular reactions of the label with chemicals in solution. The two types of reaction can be distinguished by manipulating the viscosity of the solution and/or by varying the concentration of the reductant/oxidant. Both strategies will affect the inter- but not the intramolecular kinetics and both were applied in the present study.

The dependence of the PET rate on the distance between label and Cu center was studied by choosing two positions for the label, one close to and one remote from the Cu site (at 18.5 and 29.1 Å, the label being attached at Lys122 and at the N terminus, respectively). Second, the effect of the redox activity of the metal was investigated by studying the Cu-containing protein (CuAz) next to the (redox inactive) Zn-containing variant (ZnAz). Finally, the effect of the redox state of the Cu on the PET reaction was explored by studying labeled azurin in the oxidized and the reduced form.

The results presented here provide detailed insight into the kinetics of intra- and intermolecular PET reactions. The data may be of relevance in the design of biological probes for super-resolution microscopy[24] and in the analysis of the fluorescence time traces of labelled ET proteins and redox enzymes in mechanistic and structural studies.

Results

Fluorescence correlation spectroscopy

For the acquisition of the FCS data 80 μL of the sample solution was deposited onto a glass slide, and covered to avoid evaporation. Time traces were recorded for durations varying from 5 to 10 minutes and stored as time-tagged time-resolved (t3r) data files. For further details see the Supporting Information. The autocorrelation functions (ACFs) were calculated from the t3r files with the help of the SymPhoTime software (PicoQuant GmbH, Berlin, Germany).[25] The ACFs were analyzed by fitting to the following equations [Eq. (1)]:[19,26]

$$G(\tau) = G(0) \times G_{\text{diff}}(\tau) \times \prod_i G_i(\tau) \quad (1)$$

with [Eq. (2)]:

$$G(0) = \frac{1}{< N >} = \frac{1}{c \cdot V_{\text{eff}} \cdot N_{\text{A}}} \quad (2)$$

and $< N >$ the average number of particles in the probe volume, c the sample concentration, V_{eff} the effective probe volume, and N_{A} Avogadro's constant. V_{eff} amounted to 1.1–2.3 fL depending on conditions (see the Supporting Information for details).

$G_{\text{diff}}(\tau)$ relates to the diffusion of molecules in solution, and $G_i(\tau)$ relates to zero-order reactions such as fluorophore blinking and deprotonation or electron transfer (ET) reactions.[19,26] $G_{\text{diff}}(\tau)$ and $G_i(\tau)$ are given by Equations (3) and (4):[19,26]

$$G_{\text{diff}}(\tau) = \left(1 + \frac{\tau}{\tau_{\text{D}}}\right)^{-1} \left(1 + \frac{\tau}{k^2 \tau_{\text{D}}}\right)^{-\frac{1}{2}} \quad (3)$$

$$G_i(\tau) = \frac{\left(1 - F_i + F_i e^{-\tau/\tau_i}\right)}{(1 - F_i)} \quad (4)$$

where τ_{D} is the diffusion correlation time of the molecule, k is the structure parameter, τ_i is the correlation time of the ith independent zero-order reaction, and F_i is the corresponding fraction of molecules in the dark state (see the Supporting Information).

Most of the cases described below required the inclusion of one or two zero-order reactions, that is, $G_1(\tau)$ or $G_1(\tau)$ and $G_2(\tau)$, in the fitting procedure to obtain a satisfactory fit. Fitting was performed in GraphPad Prism 5 or 6.05 (GraphPad Inc., USA). The quality of the fits was judged by visual inspection of the residuals.

N-terminally labeled ZnAz (Nt-ZnAz), K122-labeled ZnAz (K122-ZnAz) and N-terminally labeled CuAz (Nt-CuAz) behaved in a similar way in the FCS. The results are analyzed together. K122-labeled CuAz behaved differently and the results are presented separately.

Results for Nt-ZnAz, K122-ZnAz and Nt-CuAz

Oxidizing conditions

Fluorescence time traces of solutions of Nt-ZnAz in 58% (w/w) sucrose were recorded in the presence of varying amounts (0–500 μM) of oxidant (potassium hexacyanoferrate(III)). In this and all other experiments, 10–20 different concentrations of oxidant or reductant were analyzed. An example is shown for 50 μM hexacyanoferrate(III) in Figure 1 (red curve; see also Figure S5). (Throughout the text examples of the experimental findings are provided by selected figures in the main text and/or (additional) figures in the Supporting Information. Complete data sets of all experiments available on request.)

Application of Equations (1)–(3) provides excellent fit of the data (Figures 1 and S5). As expected, under oxidizing conditions (red curve) the diffusion correlation time τ_D is independent of the $K_3Fe(CN)_6$ concentration (Figure S5.C) and amounts to 11.3(±0.6) ms. The same observation obtained for K122-ZnAz and Nt-CuAz with τ_D values in the range of 11–13 ms. These values agree within a factor of two with the estimated value (see the Supporting Information). Clearly, in these cases, the label fluorescence is not affected by the added oxidant.

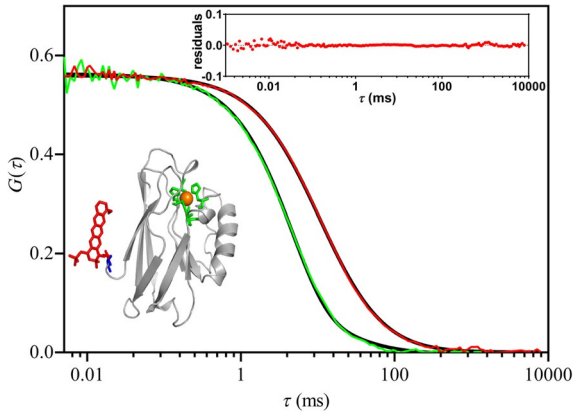

Figure 1. Autocorrelation function (ACF) of ZnAz labeled at the N terminus with ATTO655. The sample contained 50 μM of hexacyanoferrate(III) (red curve) or 500 μM of hexacyanoferrate(II) (green curve). The black lines are fits according to Equation (1) with $G(\tau)=G(0)\ G_{diff}(\tau)$ and $G(\tau)=G(0)\ G_{diff}(\tau)\ G_1(\tau)$, respectively. The inset at the top shows the residuals of the fit for the red curve. The residuals for the green curve are similar. The inset at the bottom is a cartoon of N terminally labeled azurin. The label is depicted in red, Cu in orange and the Cu ligands in green.

Reducing conditions

The observations were different under reducing conditions. The data for Nt-ZnAz titrated with potassium hexacyanoferrate(II) were fitted with Equations (1)–(3) (only accounting for diffusion) but the residuals exhibited a noticeable non-random component) and, more importantly, the diffusion time, τ_D, varied strongly with hexacyanoferrate(II) concentration (Figure S6). Therefore, the ACFs were fit with an equation containing a diffusion term and a single blinking term ($G(\tau)=G(0)\ G_{diff}(\tau)\ G_1(\tau)$ [Eqs. (1)–(4)] with the diffusion correlation time fixed at $\tau_D=12$ ms. Satisfactory fits were obtained now (Figure 1; green curve). Interestingly, the values of τ_1 and F_1 [see Eq. (4)] varied with reductant concentration (Figure 2A). Use of ascorbate as a reductant gave similar results (Figure S7). For K122-ZnAz and Nt-CuAz similar observations applied (Figures S8 and S9).

The variation in F_1 and τ_1 with reductant concentration can be analyzed assuming that the label undergoes transitions between a bright and a dark state with rate constants k_f for the transition from bright to dark and k_b for the reverse transition. Expressions for F_1 and τ_1 in terms of k_f and k_b are[21] $F_1=k_f/(k_f+k_b)$ and $\tau_1=(k_f+k_b)^{-1}$.

The dependence of $k_f=F_1/\tau_1$ and $k_b=(1-F_1)/\tau_1$ on reductant concentration is illustrated by Figures 2B and C for Nt-ZnAz. It is clear that k_f depends linearly on reductant concentration. We ascribe the corresponding reaction to the one electron reduction of the excited label by the reductant.[17] The expression for k_f then is [Eq. (5)]:[27]

$$k_f = k_r[R]\frac{k_{01}}{k_{10}+k_{01}} \equiv k_r[R]f(I) \qquad (5)$$

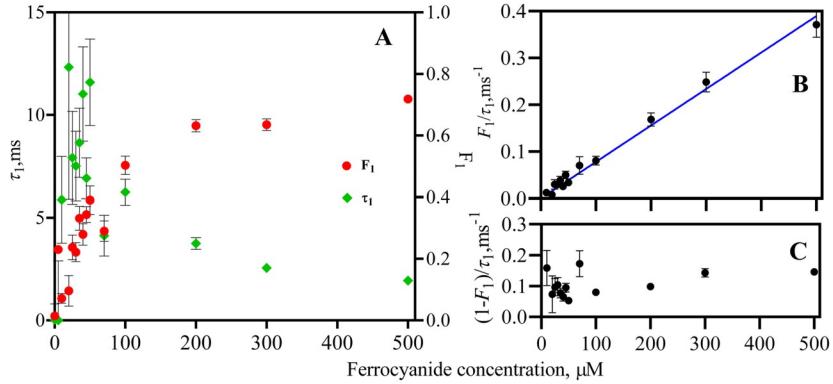

Figure 2. Parameters obtained from the analysis of the ACFs of N-terminally labeled Zn azurin. ACFs were fitted with the equation $G(\tau)=G(0)\ G_{diff}(\tau)\ G_1(\tau)$ with τ_D fixed at 12 ms. A) Parameters τ_1 and F_1, as obtained from the fits, as a function of the concentration of added hexacyanoferrate(II). Vertical bars here and elsewhere indicate 95% confidence intervals. Towards lower reductant concentration the contribution of $G_1(\tau)$ to the ACF diminishes and becomes less well defined, which is reflected in increasing confidence intervals. B) F_1/τ_1 ($=k_f$); the straight line is a least squares fit to the data points. C) $(1-F_1)/\tau_1$ ($=k_b$).

k_r is the second-order rate constant for the reaction of the reductant with the excited label, [*R*] is the concentration of reductant, $k_{01} = \sigma I_{exc}$, with σ the absorption cross section of the label at the wavelength of the laser, I_{exc} the laser power in terms of number of photons $s^{-1} cm^2$; k_{10} is the decay rate of the excited state. The factor *f*(*I*) represents the steady state fraction of molecules in the excited state.[27] The dependence of *f*(*I*) on I_{exc} was checked by measuring k_f as a function of the excitation light intensity (see the Supporting Information and Figure S10). The slope of a graph of k_f versus [*R*] (Figure 2B) provides a value of $k_r f(I)$, which amounted to $(7.8 \pm 0.2) \times 10^5$ $M^{-1} s^{-1}$ ($(2.8 \pm 0.2) \times 10^5$ $M^{-1} s^{-1}$ when ascorbate was used as a reductant). Similar behavior is observed for K122-ZnAz and Cu-containing Nt-CuAz. Data are gathered in Table 1.

From the experimentally determined value of $k_r f(I)$ a value of k_r can be extracted with an estimate of *f*(*I*). With a fluorescence life time of 2.7 ns (measured in sucrose solution), an incident light intensity of 4.3 kW cm^{-2} at 636 nm (vide supra), and an absorbance cross section of the label of 1.3×10^{-16} cm^2 (based on an estimated $\varepsilon_{636} = 8 \times 10^4$ M^{-1} cm^{-1}), one finds $\sigma I_{exc} = 1.80 \times 10^6$ s^{-1} and $f(I) = 4.8 \times 10^{-3}$. Taking N-terminally labeled ZnAz reduced by cyanoferrate(II) as an example, with $k_r f(I) = (7.8 \pm 0.2) \times 10^5$ $M^{-1} s^{-1}$ (see above) one finds $k_r = (1.6 \pm 0.1) \times 10^8$ $M^{-1} s^{-1}$. This rate is compatible with a diffusion-controlled reaction in a high viscosity medium (58% w/w sucrose solutions, see the Supporting Information).

As for the back reaction (Figure 2C), it appears that k_b is independent of the concentration of reductant, consistent with the idea that oxygen is responsible for the back oxidation. Oxygen is present in large excess and its concentration will not change appreciably over the duration of the experiment. The average value of k_b is listed in Table 1. When assuming that the reaction is second order with rate k_0, one finds with $k_b = (9.5 \pm 0.4) \times 10^1$ s^{-1} (Figure 2C, Table 1) and $[O_2] \approx 260$ μM (aerobic solution) that $k_0 = (0.4 \pm 0.1) \times 10^6$ $M^{-1} s^{-1}$ indicating that many encounters between the reactants are required before an oxidation event takes place. Rate constants for K122-ZnAz and Nt-CuAz in the presence of reductant were obtained in the same way and are collected in Table 1.

Results for K122-CuAz

Oxidizing conditions

When titrating K122-CuAz with hexacyanoferrate(III) a two-term function with $G_{diff}(\tau)$ and $G_1(\tau)$ was needed to fit the ACFs properly (Figure S11). Both F_1 and τ_1 appeared independent of the ferricyanide concentration with $F_1 = 0.17 \pm 0.01$ and $\tau_1 = 1.1(\pm 0.2)$ ms (Figure 3).

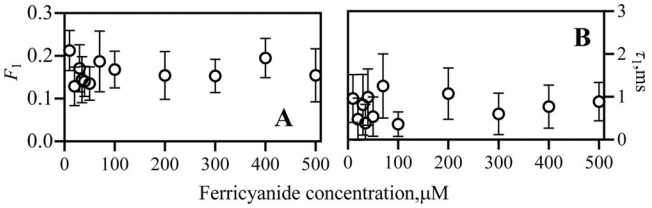

Figure 3. Parameters F_1 (A) and τ_1 (B) obtained by fitting the ACFs of Cu azurin labeled at Lys122 with $G(\tau) = G(0)\ G_{diff}(\tau)\ G_1(\tau)$ (with $\tau_D = 12$ ms) as a function of the concentration of added hexacyanoferrate(III).

It is clear, therefore, that next to the diffusion term, a blinking term is needed to fit the experimental ACF properly. This blinking reaction was not observed in the case of the Zn containing K122-labeled protein and so the Cu center must be involved in this reaction. Moreover, the blinking is also absent in the N-terminally labeled CuAz, which must mean that the distance between the Cu and the label is a critical factor (29.1 Å for Nt-Az vs. 18.5 Å for K122-Az). These are strong indications that intramolecular ET from the excited label to the Cu^{II} site, and back, is responsible for the observed blinking, according to Scheme 1. Consistent with the intramolecular character of

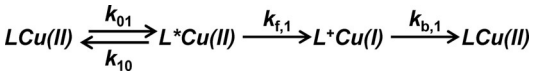

Scheme 1. Light induced ET reactions in oxidized CuAz following optical excitation of the label, *L*. *LCu* symbolizes the labeled azurin molecule in which the Cu is in the reduced or oxidized form (Cu^I or Cu^{II}, respectively) and the label, *L*, is excited or oxidized (*L** or L^+, respectively). The rates for intramolecular ET from *L** to Cu^{II} and from Cu^I to L^+ are denoted by $k_{f,1}$ and $k_{b,1}$, respectively.

Table 1. Experimental inter- and intramolecular ET rate constants. See text for details.

Intermolecular ET	Label at	$k_r f(I)$ [$M^{-1} s^{-1}$][a]	$k_r f(I)$ [$M^{-1} s^{-1}$][b]	k_b [s^{-1}][a]	k_b [s^{-1}][b]
ZnAzurin	N terminus	$(7.8 \pm 0.2) \times 10^5$	$(2.8 \pm 0.2) \times 10^5$	$(9.5 \pm 0.4) \times 10^1$	$(3.1 \pm 0.2) \times 10^1$
	K122	$(6.2 \pm 0.1) \times 10^5$	$(3.3 \pm 0.2) \times 10^5$	$(4.8 \pm 0.2) \times 10^1$	$(4.1 \pm 0.1) \times 10^1$
CuAzurin	N terminus	$(7.0 \pm 0.4) \times 10^5$	$(3.2 \pm 0.3) \times 10^5$	$(4.2 \pm 0.1) \times 10^1$	$(3.5 \pm 0.2) \times 10^1$
	K122	$(4.2 \pm 0.3) \times 10^5$	$(2.0 \pm 0.3) \times 10^5$	$(9.7 \pm 0.9) \times 10^1$	$(5.6 \pm 0.6) \times 10^1$
Intra-molecular ET	Label at	$k_{f,1}$ [s^{-1}][c]	$k_{b,1}$ [s^{-1}][c]	$k_{f,2}$ [s^{-1}]	$k_{b,2}$ [s^{-1}]
CuAzurin	K122	$(4.8 \pm 0.3) \times 10^4$	$(0.7 \pm 0.1) \times 10^3$	$(3.3 \pm 0.7) \times 10^{6[d]}$	$(1.0 \pm 0.2) \times 10^{4[d]}$
		–	–	$(2.2 \pm 0.1) \times 10^{6[e]}$	$(1.4 \pm 0.1) \times 10^{4[e]}$

[a] Reductant: hexacyanoferrate(II). [b] Reductant: ascorbate. [c] In the presence of excess of hexacyanoferrate(III). [d] In the presence of excess of ascorbate. [e] In the presence of excess of hexacyanoferrate(II).

the reaction, neither F_1 nor τ_1 were found to depend on the concentration of oxidant (Figure 3).

Following the same formalism as applied above for ZnAz one obtains $F_1/\tau_1 = f(I)$ and $(1-F_1)/\tau_1 = k_{b,1}$.

In oxidized azurin, the label fluorescence is partly quenched by the Cu center and the fluorescence lifetime is shortened to 1.8 ns leading to $f(I) = 3.2\times10^{-3}$. With $F_1 = 0.17(\pm0.01)$ and $\tau_1 = 1.1(\pm0.2)$ ms, one obtains $k_{f,1} = (4.8\pm0.3)\times10^4\ s^{-1}$ and $k_{b,1} = (0.7\pm0.1)\times10^3\ s^{-1}$. Data are collected in Table 1.

Reducing conditions

Under reducing conditions evidence for an additional fluorescence decay term appeared in the ACF of K122-CuAz in the sub-millisecond time range (Figure 4; data for ascorbate shown) and only the use of a three-term correlation function [Eqs. (1)–(4)], with $G_1(\tau)$ and $G_2(\tau)$, and with τ_D fixed at 12 ms) resulted in satisfactory fits.

The amplitudes F_1 and F_2, and the corresponding correlation times, τ_1 and τ_2 are presented in Figure 5 as a function of ascorbate concentration. Similar results were obtained with the use of hexacyanoferrate(II) (see Figure S12).

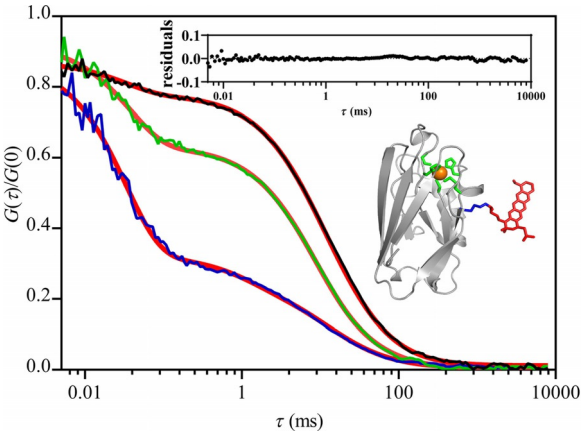

Figure 4. ACFs of CuAz labeled at K122 with ATTO655 containing 5(black), 55(green) and 500(blue) μM of ascorbate. The red lines are fits according to $G(\tau) = G(0)\ G_{diff}(\tau)\ G_1(\tau)\ G_2(\tau)$ (with $\tau_D = 12$ ms). The traces have been normalized for clarity of presentation. The inset at the top is a graph of the residuals corresponding to the black colored ACF. The residuals of the other two curves (not shown) are similar. The inset at the right is a cartoon of K122-labeled azurin color coded as in Figure 1.

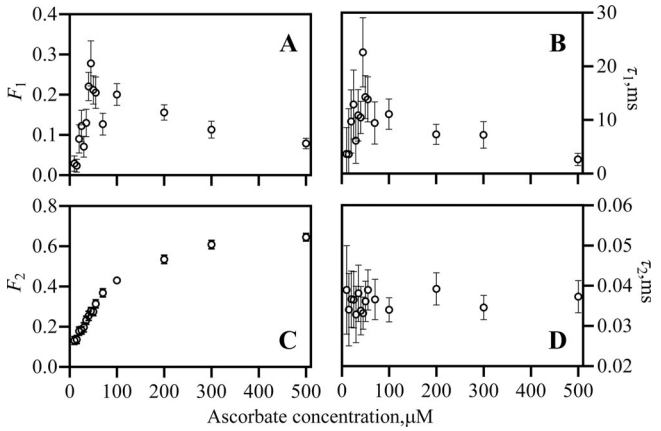

Figure 5. Parameters obtained by fitting the ACFs of CuAz labeled on K122 with $G(\tau) = G(0)\ G_{diff}(\tau)\ G_1(\tau)\ G_2(\tau)$ (with $\tau_D = 12$ ms) as a function of the ascorbate concentration: A) F_1, B) τ_1, C) F_2, and D) τ_2.

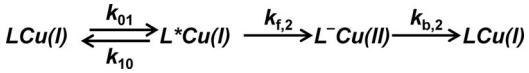

Scheme 2. Light-induced ET reactions in reduced CuAz following optical excitation of the label, *L*. Symbols have the same meaning as in Scheme 1. The rates for intramolecular ET from Cu^I to L^* and from L^- to Cu^{II} are denoted by $k_{f,2}$ and $k_{b,2}$.

As is clear from Figures 4 and 5, K122-labeled CuAz is involved in a reaction (corresponding with $G_2(\tau)$) that occurs on a time scale of 10–100 μs. Similar to the preceding case this reaction is ascribed to intramolecular ET, this time from the Cu^+ site to the excited label and back (Scheme 2).

Again, consistent with the intramolecular character of the reaction, τ_2 appears independent of the reductant concentration (Figure 5D). What seems at variance with this explanation is that the fraction of dark molecules F_2, increases with reductant concentration (Figure 5C). We ascribe this to the oxygen present in the solution. [It was found that removing the oxygen from solutions of pure ATTO655 resulted in severe blinking of the dye. Similar observations applied for solutions of labeled azurin.] When reductant is introduced into the solution in small amounts it will be partly oxidized which results in incomplete reduction of azurin. However, the ratio between reduced and oxidized protein will gradually increase as more and more reductant is added. As explained in the introduction, oxidized and reduced azurin exhibit different brightness and when both are present in the solution, the expression for the ACF has to be slightly modified according to Equation (6) (see the Supporting Information for details):

$$G(\tau) \propto \frac{1}{<N>} G_{diff}(\tau) G_1(\tau)\left(1 + \beta K e^{-\tau/\tau 2}\right) \qquad (6)$$

with $K = F_{2,red}/(1-F_{2,red})$ and $0 \le \beta \le 1$ depending on the ratio between oxidized and reduced azurin. For a 100% reduced or 100% oxidized solution β equals 1 or 0, respectively.

Equation (6) is similar to the Equations (1)–(4) that were used to fit the data of K122-labeled CuAz in Figure 4, except for the factor β. Thus, F_2 as obtained from the fits is not constant because the fit equation did not contain β, which varies with the redox potential of the solution. The experimental setup did not allow for the precise control of β. However, assuming that at 500 μM of reductant, β is close to its asymptotic value of 1, it follows that $K = F_2/(1-F_2) = 1.5\pm0.3$ (Figure 5C). Applying the same analysis as before one obtains $\mathbf{F}_2/\tau_2 = f(I)\ k_{f,2}$ and $(1\text{-}F_2)/\tau_2 = k_{b,2}$; with $F_2 = 0.6\pm0.1$, $\tau_2 = 38\pm6$ μs and $f(I) = 4.8\times10^{-3}$ one finds $k_{f,2} = (3.3\pm0.7)\times10^6\ s^{-1}$ and $k_{b,2} = (1.0\pm0.2)\times10^4\ s^{-1}$.

The data obtained with hexacyanoferrate(II) instead of ascorbate (Figure S12A) were analyzed similarly (Figures S12B–E). The resulting intramolecular ET rates are presented in Table 1.

Finally, $G_1(\tau)$ is related to the reduction of the label by the reductant and τ_1 and F_1 are analyzed as before, taking into account that only a fraction $(1-F_2)$ of the molecules is in the bright state, this time. The analysis is presented in the Supporting Information (Figure S13) and data are gathered in Table 1.

Discussion

Marcus analysis

It is of interest to consider the measured intramolecular ET rates in more detail. The framework for the analysis is provided by Marcus' theory according to which, the rate of transfer of an electron from a donor *D* to an acceptor *A*, k_{ET}, is given by [Eq. (7)]:[28]

$$k_{ET} = \frac{2\pi}{\hbar}\frac{H_{DA}^2}{\sqrt{4\pi\lambda k_B T}}\, e^{-\frac{(\Delta G+\lambda)^2}{4\lambda k_B T}} \qquad (7)$$

Here H_{DA} represents the electronic coupling matrix element between donor and acceptor, λ is the reorganization energy and ΔG is the driving force for electron transfer, with the other symbols having their usual meaning. The bridge that connects *D* and *A* provides a pathway for ET and the coupling of donor and acceptor with the bridge and the coupling between the elements of the bridge determine H_{DA}.[29–31] In the present case, two pathways may be operational. A covalent pathway is provided by the protein and the linker that connects the dye with the protein. An additional "through space" pathway may obtain when the dye forms an association (van der Waals) complex with the protein. Both pathways may contribute to H_{DA}.

Effect of optical excitation

To obtain an idea on how optical excitation of the label might affect H_{DA} and λ, TD-DFT calculations were performed on ATTO655 as well as the chromophore of this system, oxazine-1 (see the Supporting Information). Comparison of the Mulliken populations in the ground state and the lowest excited singlet state shows that the changes in charge density upon excitation are small (see the Supporting Information). Also, the off-diagonal Mulliken population between C17 and N15 (which is where the aliphatic linker and ATTO655 are connected), shows only a minimal change (less than 2%) upon excitation. Thus, it may be concluded that the electron exchange between chromophore and aliphatic linker, and thereby the through-bond contribution to H_{DA}, will virtually not be affected by the optical excitation. For through-space pathways we expect the same.

The reorganization energy can be decomposed into an inner shell and an outer shell contribution.[28] To assess the inner shell contribution we have performed TD-DFT calculations on the vertical and adiabatic ionization energies and electron affinities of the electronic ground state and of the lowest excited singlet state of the oxazine. The data show (see the Supporting Information under Intramolecular reorganization energies) that the intramolecular reorganization energies for forward and backward ET differ by no more than 0.1 eV. Furthermore, we find no indications that the promoting skeletal modes that are used in some formulations of Marcus' theory[32–34] are sizably affected upon excitation, ionization, or reduction. The outer shell contribution is dominated by the interaction with the solvent and is often estimated with the help of Marcus' dielectric continuum model[28]. Here, the orientation and distribution of the solvent molecules around donor and acceptor are assumed to be in thermal equilibrium. When the chromophore is in the ground state this condition applies naturally; for *L** it will be fulfilled since the relaxation time of the water molecules is much shorter than the fluorescence lifetime of the dye (ps vs. ns). Consequently, within the framework of the dielectric continuum model the reorganization energies for ET to or from *L* and *L** will be similar. Thus, of the three parameters in Equation (7), that is, ΔG, H_{DA} and λ, only ΔG will be sizably affected by optical excitation of the chromophore.

Reducing conditions

Intramolecular ET was observed for K122-CuAz under oxidizing as well as reducing conditions. The latter case is considered first. Applying Equation (7) and assuming similar reorganization energies and electronic coupling elements for the forward and backward ET reactions one obtains [Eq. (8)]:

$$\ln(k_{2,f}/k_{2,b}) = [(\Delta G_b+\lambda)^2-(\Delta G_f+\lambda)^2]/(4\lambda kT) \qquad (8)$$

with ΔG_f and ΔG_b the driving forces for the forward and backward ET reactions, respectively. ΔG can be estimated with the Rehm–Weller Equation (9):[35]

$$\Delta G = eE_{D^+/D} - eE_{A/A^-} - \Delta G_{0.0} + (n_A - n_D - 1)\frac{e^2}{\varepsilon d} \qquad (9)$$

which describes the driving force ΔG for the ET by a donor (D) to an acceptor (A) with $E_{D^+/D}$ and eE_{A/A^-} denoting the midpoint potentials of donor and acceptor, respectively. Here, either the donor or the acceptor is optically excited with $\Delta G_{0,0}$ denoting the energy of the corresponding 0–0 transition. In Equation (9) *e* denotes the electronic charge, *d* the distance between donor and acceptor, ε the dielectric constant, and n_A and n_D the charges of acceptor and donor in units of $|e|$, respectively.[35] For the reduction potential of ATTO655 usually the reduction potential of the dye MR121 is used (−0.42 V vs. saturated calomel electrode, SCE)[10] However, the latter value was determined in a non-aqueous organic solvent (acetonitrile). Moreover, MR121 has a slightly different structure than ATTO655. We therefore determined the aqueous reduction potential of ATTO655 when covalently attached to azurin directly by cyclic voltammetry (see the Supporting Information). The following values were used in Equation (9): $E_{ATTO/ATTO^-} = -0.182$ V (vs. standard hydrogen electrode, SHE), and $\Delta G_{0,0} = 1.86$ eV.[10] The charges on label and Cu are $n_{ATTO} = 0$ and $n_{Cu^I} = 1$. The midpoint potential of azurin at pH 7 is 0.31 V (vs. NHE).[36,37] The values chosen for *d* and ε were $d = 10$ Å and $\varepsilon = 10$, respectively (see the Supporting Information). This leads to $\Delta G_f =$

-1.67 eV and $\Delta G_b = -0.19$ eV for the reactions shown in Scheme 2. Insertion into Eq. (8) and solving for λ leads to $\lambda =$ 1.16 eV. This value is slightly higher than the theoretically expected value (0.95 eV) given by the average of the known reorganization energies of ATTO655 and azurin (1.2 eV[38] and 0.7 eV,[39] respectively). Inserting the values obtained for $k_{2,f}$, ΔG_f and λ into Equation (7) one obtains $H_{DA} = 0.51$ cm^{-1}.

One may ask how critical is the assumption of similar reorganization energies and electronic couplings for the outcome of the calculations. It appears that relaxing this condition does affect the calculated parameters but not to a great extent. For instance, allowing H_{DA} to be different for the forward and back ET reactions by a factor of 2 affects the calculated value of λ by less than 60 mV. And setting $|\lambda_f - \lambda_b| = 0.1$ eV instead of $=$ 0 eV affects the calculated value of H_{DA} by less than 0.2 cm^{-1}.

Oxidizing conditions

The rates observed under oxidizing conditions can be analyzed in the same way. With $E_{ATTO^+/ATTO} = 1.55$ V (vs. NHE; see the Supporting Information), $n_{ATTO} = 0$ and $n_{Cu^{II}} = 2$ and the same values as above for the other parameters one obtains $\Delta G_f = -0.476$ eV, $\Delta G_b = -1.384$ eV and $\lambda = 0.76$ eV. The latter value is slightly less than the theoretically expected value (0.95 eV). Finally one finds $H_{DA} = 0.21 \times 10^{-1}$ cm^{-1}.

Pathways

It is of interest to see if the experimental ET rates concur with theoretical predictions. Various models have been proposed to calculate through-bond couplings. An ab initio calculation is outside the scope of the present study but the pathway model of Beratan and Onuchic provides an order of magnitude estimate of k_{ET} and as such has gained considerable popularity in recent years.[40] The model calculates H_{DA} by charting a path, mainly along covalent bonds, from donor to acceptor. Each step along the path attenuates the coupling by a pre-determined factor. H_{DA} is proportional to the product of these factors, the total product being denoted by the dimensionless parameter T_{DA} (see the Supporting Information for details). A customary expression for k_{ET} is given in Equation (10):[9,41,42]

$$k_{ET} = 3.10^{13}\ {T_{DA}}^2\ \exp-[(\Delta G + \lambda)^2/(4\lambda kT)] \qquad (10)$$

Using the values of ΔG, k_{ET}, and λ found (vide supra) for K122-CuAz under oxidizing and reducing conditions one finds experimental values of $T_{DA} = 0.7 \times 10^{-4}$ and 1.1×10^{-3}, respectively. The theoretical values that are calculated according to the pathway model[40] amount to 2×10^{-4}–2×10^{-3} (see the Supporting Information) depending on where the linker is considered to end and the fluorophore begins. Thus, for K122-CuAz the experimental data appear compatible with ET through a covalent pathway. For Nt-CuAz the pathway model calculates a theoretical value of $T_{DA} < 10^{-8}$ (see the Supporting Information) which means that the coupling between dye and Cu center is negligible, in accordance with the absence of observable intramolecular ET.

When the dye forms an association complex with the protein the appropriate expression for k_{ET} (sometimes denoted as the "organic glass" model) is given in Equation (11)[43]

$$^{10}\log k_{ET} = 15 - 0.6R - 3.1\ (\Delta G + \lambda)^2/\lambda \qquad (11)$$

where R is the edge to edge distance in Å between donor and acceptor and ΔG and λ are given in eV. For an estimate of R one needs detailed structural information, which is missing. We have tried to establish whether an association complex is formed between dye and protein by fluorescence polarization experiments (see the Supporting Information). It appears that the fluorescence anisotropy of the labeled protein in water ($r =$ 0.101) is less than expected when the label would be immobilized with the protein ($r = 0.145$) but longer than that of the free label ($r = 0.02$). Also the rotational correlation time of the label when attached to azurin (2.4 ns) is shorter than the rotational correlation time of azurin itself (4.75 ns). Apparently, label and protein do not form a stable complex but transient complex formation cannot be ruled out. Notably, even complete absence of complex formation would still be compatible with the fluorescence anisotropy data when fast but linker-constrained motion of the label would prevail.[44] The only inference that can be drawn at this stage is that if transient complex formation would contribute measurably to the ET rate, the lifetimes of the complexes would have to be shorter than $(k_{ET})^{-1}$, otherwise a stretched exponential instead of a single exponential decay would have shown up in the FCS curve.

Using again the values of ΔG, k_{ET}, and λ found for K122-CuAz under reducing and oxidizing conditions and inserting them into Equation (10) one finds $R = 14.0$ and 17.5 Å for the edge to edge distance, respectively. Simple molecular modelling shows that distances in this range can be attained in K122-Az–dye constructs. For Nt-CuAz R has to be > 21 Å to be compatible with the observed absence of ET which practically means that the label is not touching the protein surface and stable complex formation can be ruled out in this case.

Conclusions

The present work shows that in oxidoreductases, photo-induced intra-molecular ET between label and active center may occur over long distances. This differs from instances reported in the literature that focused on cases where van der Waals contact promotes PET.[2,10,11,38] For most oxidoreductases, van der Waals contact between label and redox center is precluded when the redox center is buried inside the protein matrix (as is the case for azurin). It is clear that for labeled oxidoreductases, PET between dye and redox center can be avoided by making the distance between them large enough, that is, distance measured either in terms of number of covalent bonds or in terms of physical distance in case of transient complex formation between label and protein. The present work shows that simple thermodynamic considerations combined with ET calculations can provide a good estimate of the chances that PET may occur, and may help in designing a labeling strategy for applications in areas like fluorescence microscopy, enzyme ki-

netics and structural studies. Furthermore, values for H_{DA} and λ reported here are in the customary range for azurin, considering the distance over which the electron transfer occurs.[8,33,34,42,45–47] With the present data at hand, it is possible to predict the dependence of the FRET and PET rates on the Cu–label distance (see Figure S14). This allows, in practice, to design systems where these distances are fine-tuned to maximize one effect over the other, depending on the requirements of the chosen application.

Experimental Section

Chemicals, proteins and sample preparation

Details about chemicals, protein preparation, purification, and labeling are provided in the Supporting Information. Samples contained 58.0% sucrose (w/w; viscosity 42.7 cP at 22 °C[48]). The final sample concentrations of labeled protein were around 0.4–0.8 nM. Manipulation of the redox potential of the solution was achieved by employing hexacyanoferrate(III), hexacyanoferrate(II) or ascorbate.

Fluorescence correlation spectroscopy setup and data acquisition

FCS experiments were performed on a home-built confocal setup equipped for time-correlated single-photon counting (TCSPC) measurements. Experiments were performed at ambient temperature (22 °C). Excitation at 639 nm was provided by a pulsed diode laser head (LDH-P-C-635-B, 20 MHz rep rate, PicoQuant GmbH, Berlin, Germany) driven by a picosecond laser driver (LDH-800-B, PicoQuant GmbH, Berlin, Germany). The power used for the calibration and for the FCS measurements amounted to 20 μW, as measured after the objective, corresponding to a specific power of $\approx$4.3 kW cm^{-2} at the sample. For the acquisition of the FCS data 80 μL of the sample solution was deposited onto a glass slide, and covered to avoid evaporation. Time traces were recorded for durations varying from 5 to 10 minutes and stored as time-tagged time-resolved (t3r) data files. For further details see the Supporting Information.

Acknowledgements

The authors gratefully acknowledge the assistance of Dr. L. C. Tabares with the building of the FCS spectrometer in the early stages of this project and of Biswajit Pradhan with the fluorescence anisotropy measurements. They thank Prof. Fred Hagen (Delft University) for his advice on the cyclic voltammetry experiments. This project was supported by the Netherlands Science Organization (NWO) with financial help by the Foundation for the Chemical Sciences (CW) through TOP grant 700.56.304 and by the European Commission through the EdRox research and training network grant MRTN-CT-2006-035649.

Conflict of interest

The authors declare no conflict of interest.

Keywords: copper protein · electron transfer · fluorescence correlation spectroscopy · FRET · redox enzymes

[1] R. Roy, S. Hohng, T. Ha, *Nat. Methods* **2008**, *5*, 507–516.
[2] H. Yang, G. B. Luo, P. Karnchanaphanurach, T. M. Louie, I. Rech, S. Cova, L. Y. Xun, X. S. Xie, *Science* **2003**, *302*, 262–266.
[3] A. Brunger, P. Strop, M. Vrljic, S. Chu, K. Weninger, *J. Struct. Biol.* **2011**, *173*, 497–505.
[4] T. Ha, P. Tinnefeld, *Annu. Rev. Phys. Chem.* **2012**, *63*, 595–617.
[5] A. Gupta, T. J. Aartsma, G. W. Canters, *J. Am. Chem. Soc.* **2014**, *136*, 2707–2710.
[6] S. Kuznetsova, G. Zauner, T. J. Aartsma, H. Engelkamp, N. Hatzakis, A. E. Rowan, R. J. M. Nolte, P. C. M. Christianen, G. W. Canters, *Proc. Natl. Acad. Sci. USA* **2008**, *105*, 3250–3255.
[7] H. Sahoo, *J. Photochem. Photobiol. C* **2011**, *12*, 20–30.
[8] J. R. Winkler, H. B. Gray, *Chem. Rev.* **1992**, *92*, 369–379.
[9] J. R. Winkler, H. B. Gray, *J. Am. Chem. Soc.* **2014**, *136*, 2930–2939.
[10] S. Doose, H. Neuweiler, M. Sauer, *ChemPhysChem* **2009**, *10*, 1389–1398.
[11] M. Sauer, H. Neuweiler, in *Fluorescence Spectroscopy and Microscopy* (Eds.: Y. Engelborghs, A. Visser) Humana, **2014**, pp. 597–615.
[12] R. Zhu, X. Li, X. S. Zhao, A. Yu, *J. Phys. Chem. B* **2011**, *115*, 5001–5007.
[13] U. Kolczak, C. Dennison, A. Messerschmidt, G. W. Canters, in *Handbook of Metalloproteins*, Wiley, **2006**, pp. 1170–1194.
[14] E. Vijgenboom, J. E. Busch, G. W. Canters, *Microbiology* **1997**, *143*, 2853–2863.
[15] H. Nar, A. Messerschmidt, R. Huber, M. van de Kamp, G. W. Canters, *J. Mol. Biol.* **1991**, *221*, 765–772.
[16] J. Vogelsang, R. Kasper, C. Steinhauer, B. Person, M. Heilemann, M. Sauer, P. Tinnefeld, *Angew. Chem. Int. Ed.* **2008**, *47*, 5465–5469; *Angew. Chem.* **2008**, *120*, 5545–5550.
[17] J. Vogelsang, T. Cordes, C. Forthmann, C. Steinhauer, P. Tinnefeld, *Proc. Natl. Acad. Sci. USA* **2009**, *106*, 8107–8112.
[18] Q. S. Zheng, M. F. Juette, S. Jockusch, M. R. Wasserman, Z. Zhou, R. B. Altman, S. C. Blanchard, *Chem. Soc. Rev.* **2014**, *43*, 1044–1056.
[19] O. Krichevsky, G. Bonnet, *Rep. Prog. Phys.* **2002**, *65*, 251–297.
[20] P. Schwille, E. Haustein, *Fluorescence Correlation Spectroscopy: An Introduction to Its Concepts and Applications, in Fluorescence Correlation Spectroscopy: Theory and Applications* (Eds.: E. L. Elson, R. Rigler), Springer, Berlin, **2001**, pp 1–33.
[21] E. Haustein, P. Schwille, *Ann. Rev. Biophys. Biomol. Struct.* **2007**, *36*, 151–169.
[22] S. Felekyan, R. Kuhnemuth, V. Kudryavtsev, C. Sandhagen, W. Becker, C. A. M. Seidel, *Rev. Sci. Instrum.* **2005**, *76*, 083104.
[23] M. Goldberg, I. Pecht, *Biochemistry* **1976**, *15*, 4197–4208.
[24] U. Bhattacharjee, C. Beck, A. Winter, C. Wells, J. W. Petrich, *J. Phys. Chem. B* **2014**, *118*, 8471–8477.
[25] P. Kapusta, M. Wahl, A. Benda, M. Hof, J. Enderlein, *J. Fluoresc.* **2007**, *17*, 43–48.
[26] J. Widengren, A. Chmyrov, C. Eggeling, P. A. Lofdahl, C. A. M. Seidel, *J. Phys. Chem. A* **2007**, *111*, 429–440.
[27] J. Widengren, R. Rigler, U. Mets, *J. Fluoresc.* **1994**, *4*, 255–258.
[28] R. A. Marcus, N. Sutin, *Biochim. Biophys. Acta* **1985**, *811*, 265–322.
[29] H. B. Gray, J. R. Winkler, *Quart. Rev. Biophys.* **2003**, *36*, 341–372.
[30] H. Mcconnell, *J. Chem. Phys.* **1961**, *35*, 508.
[31] M. D. Newton, N. Sutin, *Annu. Rev. Phys. Chem.* **1984**, *35*, 437–480.
[32] G. L. Closs, J. R. Miller, *Science* **1988**, *240*, 440–447.
[33] M. W. Holman, R. C. Liu, L. Zang, P. Yan, S. A. DiBenedetto, R. D. Bowers, D. M. Adams, *J. Am. Chem. Soc.* **2004**, *126*, 16126–16133.
[34] T. Kircher, H. G. Lohmannsroben, *Phys. Chem. Chem. Phys.* **1999**, *1*, 3987–3992.
[35] D. Rehm, A. Weller, *Isr. J. Chem.* **1970**, *8*, 259.
[36] C. S. St. Clair, W. R. Ellis, H. B. Gray, *Inorganica Chimica Acta* **1992**, *191*, 149–155.
[37] M. Van de Kamp, G. W. Canters, C. R. Andrew, J. Sanders-Loehr, C. J. Bender, J. Peisach, *Eur. J. Biochem.* **1993**, *218*, 229–238.
[38] C. A. M. Seidel, A. Schulz, M. H. M. Sauer, *J. Phys. Chem.* **1996**, *100*, 5541–5553.
[39] H. B. Gray, B. G. Malmstrom, R. J. P. Williams, *J. Biol. Inorg. Chem.* **2000**, *5*, 551–559.

[40] I. A. Balabin, X. Q. Hu, D. N. Beratan, *J. Comput. Chem.* **2012**, *33*, 906 – 910.
[41] C. C. Moser, J. M. Keske, K. Warncke, R. S. Farid, P. L. Dutton, *Nature* **1992**, *355*, 796 – 802.
[42] J. N. Onuchic, D. N. Beratan, J. R. Winkler, H. B. Gray, *Ann. Rev. Biophys. Biomol. Struct.* **1992**, *21*, 349 – 377.
[43] C. C. Moser, P. L. Dutton, *Biochimica Et Biophysica Acta* **1992**, *1101*, 171 – 176.
[44] J. R. Lakowicz, in *Principles of Fluorescence Spectroscopy*, 2nd ed., Springer, **2010**, Chapter 10, pp. 291 – 319.
[45] R. G. Hadt, S. I. Gorelsky, E. I. Solomon, *J. Am. Chem. Soc.* **2014**, *136*, 15034 – 15045.
[46] M. R. Hartings, I. V. Kurnikov, A. R. Dunn, J. R. Winkler, H. B. Gray, M. A. Ratner, *Coord. Chem. Rev.* **2010**, *254*, 248 – 253.
[47] T. R. Prytkova, I. V. Kurnikov, D. N. Beratan, *J. Phys. Chem. B* **2005**, *109*, 1618 – 1625.
[48] W. M. Haynes, D. R. Lide in *CRC Handbook of Chemistry and Physics*, 63rd ed., **2000**, pp. 1082 – 1083.

Manuscript received: August 9, 2017
Accepted manuscript online: October 24, 2017
Version of record online: December 6, 2017